Chapter IV

Photocatalytic activity of the nanoscale WS_2 against harmful pollutants

4.1 Target dyes and role of photocatalysis

All around the globe, researchers are trying hard to find effective means and measures to degrade harmful organic dyes and pollutants available in the environment. Like graphene, WS_2 comes with a two dimensional (2D) layered conformation, and the latter is capable of exhibiting a sizable band gap that can also be tuned [1]. Because of the atomically thin layered structure, it has got large surface- to- volume ratio and thus, enriched with numerous reactive sites [2]. This allows the nanoscale WS_2 to act as an advanced photocatalytic agent as compared to the traditional photocatalysts, such as TiO_2, SnO_2 and ZnO, which are generally efficient only under UV light irradiation [3]. Researchers have explored the photocatalytic performance of WS_2 in different morphologies and also in composite form with other suitable candidates [4, 5]. In the past, there has always been some effort to enhance the photocatalytic efficiency of WS_2, MoS_2 and related compounds [4, 5]. In the present chapter, we shall discuss the photocatalytic performances of IF type WS_2 nanoparticles, WS_2 nanosheets system under UV light and visible light illumination considering malachite green (MG) as the target dye. We have also investigated the photocatlytic efficiency of WS_2/C-dot nanosheets under visible light taking and methyl orange (MO) as the target dyes.

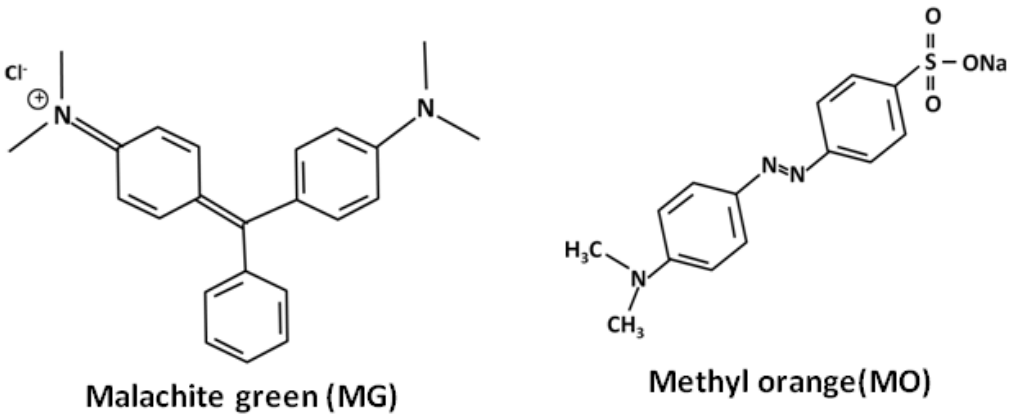

Figure 4.1: Molecular structure of the harmful organic dyes

The MG is an organic compound that is used as a dyestuff and controversially, as an antimicrobial agent in aquaculture [6]. In contrast, the MO dye is regarded as a pH indicator in the titration process because of its precise colour variance with pH [7]. While researchers across the globe putting numerous effort to tackle the associated problems due to harmful dyes and pollutants, there is no single most short-cut approach to address the critical environmental issues realised at present. Consequently, advanced materials with diverse morphologies and dimensions are always welcome in this area of research and development. Herein, photocatalytic activities of nanoscale-WS_2 have been examined and analyzed.

4.2 Photocatalytic activity of IF-type WS_2 nanoparticles and WS_2 nanosheets

The photoactivity of the nano-WS_2 samples has been investigated both under UV and day light illumination conditions. To perform the experiment with IF-type WS_2 nanoparticles, 100 mg/L of the WS_2 nanoparticles is first added to 30 mg/L of the MG, and then subjected to stirring for about 1 h in the dark environment. In the next step, the mixture is ultrasonicated for about half an hour. The collected sol is then placed inside a cabinet which has the provision for the UV lamp as well as the incandescent lamp, the latter being used as the source of visible light. The samples are placed at the base of the chamber at a distance of 12 cm from the UV source (λ = 365 nm) and the polychromatic visible light source used independently. The WS_2 nanocatalyst-loaded dyes were irradiated for 15, 30, 45, 60 and 120 min. Next, 5 ml of the MG solution is taken for optical absorption analysis, knowing that the peak maximum for the initial absorption of MG appears at ~617 nm [8]. The same method is applied to examine the photocatalytic efficiency of WS_2 nanosheets. As for the nanosheets, the amount of nanocatalyst taken was 60 mg/L while the amount of MG was fixed at 20 mg/L. The WS_2 nanosheet loaded dyes were irradiated for 15, 30, 45 and 60 min. The percentage of decomposition of the MG under UV and visible light irradiation for various durations of UV exposure is given by:

$$\% \text{ degradation} = \frac{C_0 - C_t}{C_0} \times 100\ \% \qquad (4.1)$$

where C_0 and C_t represent concentration of either MG solution before and after irradiation [9].

Upon light irradiation, the WS_2 nanocatalysts are believed to be photo-excited releasing electrons and holes. The electrons are lifted to the conduction band leaving behind holes in the valence band. The *e*–*h* pairs are likely to be captivated in the active W^{4+} and S^{2-} defect sites, otherwise, it is likely that recombination of these carriers would take place to dissipate energy [10]. These carriers would migrate to the nanocatalyst surfaces, resulting in the formation of intermediate reactants. The light-induced holes and the reactive hydroxyl radicals are extremely important for the stimulation of the redox reaction necessary for decomposition of water. The target MG, being in aqueous form, the water molecule is believed to come in contact with the surfaces of the nanocatalyst. The active sites of the nanocatalyst readily trap the OH group, or superoxide O^{2-}, latter being a consequence of the electrons being transferred to the adsorbed oxygen [11]. Water and hydroxyl groups are transformed to hydroxyl radicals by the photogenerated holes. The superoxide and hydroxyl radicals are readily responsible for the decomposition of the organic dyes into the harmless entities/products [12]. This is schematically depicted in Fig. 4.2.

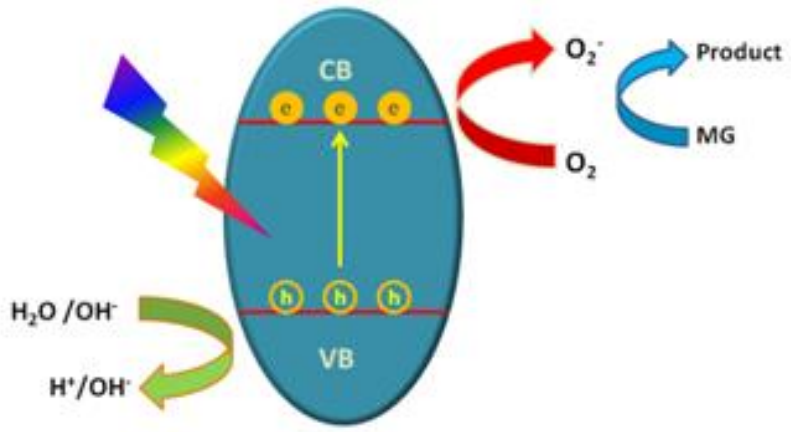

Figure 4.2: Schematic of the photocatalytic mechanism expected in the nano-WS_2 system.

The relevant chemical reactions involved in the photocatalysis process are as given below [2]:

$$WS_2 + hv \rightarrow e^- + h^+ \quad (4.2)$$

$$h^+ + H_2O \rightarrow H^+ + OH \cdot \quad (4.3)$$

$$e^- + O_2 \rightarrow O_2^- \quad (4.4)$$

$$2e^- + O_2 + 2H^+ \rightarrow H_2O_2 \quad (4.5)$$

$$e^- + H_2O_2 \rightarrow OH \cdot + OH^- \quad (4.6)$$

To investigate photoactivity of the IF WS_2 nanoparticles, we have chosen MG as the target agent to be examined under UV and visible light illumination conditions. The UV–Vis absorption response of the organic dye and nano-WS_2 catalyst-loaded MG can be found in Fig. 4.3 (a). The WS_2-loaded dye showed a steady fall in the absorbance with increasing the UV exposure time, exhibiting a minimal strength at ~617 nm. Conversely, the samples irradiated under visible light showed a rapid drop in the absorbance response as compared to the samples subjected to the UV light (Fig. 4.3 (a), (b)). The IF-type WS_2 nanoparticles tend to exhibit better catalytic efficiency under visible light because of the narrow band gap, which acts as a driving force to activate the redox reaction necessary for the production of hydroxyl radicals [13]. Also, it has been reported that irregular hexagonal-type structures with ample surface defects served the purpose of a good nanocatalyst under visible light illumination [14]. Also, IF-type particles can have enhanced photocatalytic responses because of the strong optical absorption, large surface area, and chemical inertness under illumination.

We observed an increasing trend of degradation of the MG on increasing the irradiation time. As high as 45% decomposition has been witnessed upon exposure of the catalyst loaded dye to UV light, for 120 min (Fig. 4.3 (c)). Conversely, the IF-WS_2 nanocatalyst gives a superbly enhanced decomposition of MG (~71.2%) when subjected to visible light irradiation, considering similar exposure time duration (Fig. 4.3 (c)).

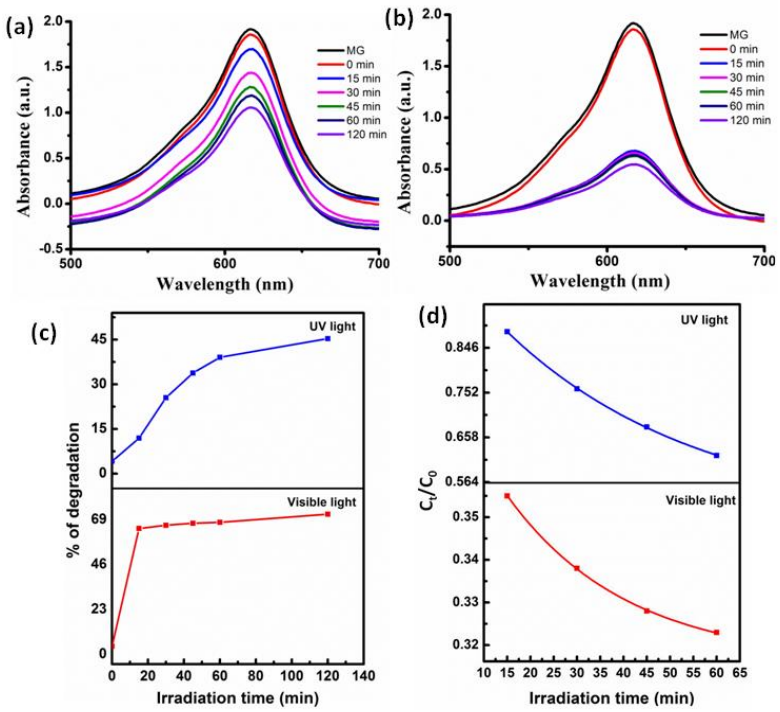

Figure 4.3: UV–Vis absorption spectra of MG and IF nano-WS_2 catalyst-loaded dye with different irradiation times: (a) UV illumination, (b) visible light illumination. The respective percentage of degradation and pseudo-first-order plots under the aforesaid conditions are shown in (c) and (d) on a comparative basis.

The performance of IF-type WS_2 nanosystem on the degradation of MG dye is evaluated through the simple kinetics, as discussed below. The kinetics of photocatalytic degradation of MG at the nanocatalyst surfaces can be understood through the Langmuir–Hinshelwood (L-H) model [15]. For a dilute solution (mM) (C<<1), it can be expressed in the form of a first-order reaction given by [15], $C_t = C_0 e^{-k_a t}$.

Here, C_0 is the initial concentration of the MG solution, t is the irradiation time and k_a is the pseudo-first order rate constant. At $t = t_0$, $C = C_0$, the initial concentration of the target before irradiation. The percentage degradation of MG is represented in Fig. 4.3 (c). The plots of C_t/C_0 versus t, for UV and visible light conditions are shown in Fig. 4.3 (d). The plots essentially help to predict the pseudo-first-order rate constant, k_a. The rate constants, as obtained directly from the graphs (Fig. 4.3 (d)), are calculated to be 0.0239 and 0.0414 min^{-1} as for the IF–type nano-WS_2 samples exposed to the UV light and visible light, respectively. A higher rate constant for the latter case, suggests that our IF-type nano-WS_2 are

capable of displaying an improved photoactivity under visible light illumination over UV light exposure.

The photocatalytic performance of the WS_2 nanosheets is also examined on the harmful organic dye (MG). The extent of degradation was observed under both UV and visible light illumination and for different durations of time. With an increase in time duration of the UV exposure, the WS_2 nanosheet-loaded dye showed a steady fall in the absorption response at λ = 619 nm (Fig. 4.4 (a–c)). We also observed a rapid fall in the absorbance under visible light illumination (Fig. 4.4 (d–f)). In other words, the WS_2 nanosheets tend to exhibit a better catalytic efficiency under visible light. This is because of its narrow band gap, which acts as a facilitator to activate the redox reaction necessary for the production of hydroxyl radicals which eventually, play a vital role in the overall photocatalytic activity.

The characteristic photocatalytic features, shown in Fig. 4.4 (a–f), suggest an increase in photodegradation of the MG with irradiation time duration, notably, with an exposure time of 60 min. The WS_2 nanosheets, under UV illumination, give as high as 67.4% decomposition of MG. But the nanocatalyst under visible light could decompose as high as, 86.6% of the MG dye. Thus, the photoactivity of the WS_2 nanosheets, owing to its relatively higher specific surface area, is drastically enhanced as compared to its IF-type counterpart.

Table 4.1: Comparison of photocatalytic activity of the systems under study

System	Target dye	Light source	Rate constant	% degradation
IF-WS_2 nanoparticles	MG	UV	0.0239	45 (120 min)
	MG	Visible	0.0414	71.2 (120 min)
WS_2 nanosheets	MG	UV	0.11	67.4 (60 min)
	MG	Visible	0.16	86.6 (60 min)
WS_2/C-dot nanohybrid	MO	Visible	0.0215	81.2 (60 min)
	MG	Visible	0.168	91 (60 min)

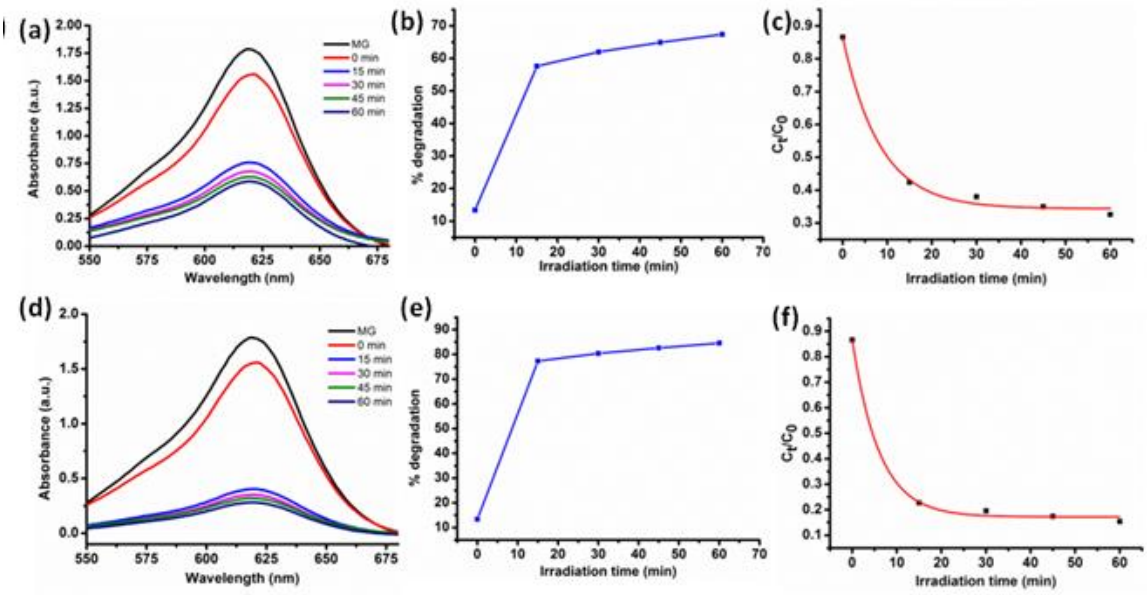

Figure 4.4: UV–Vis optical absorption spectra of MG and WS_2 nanocatalyst (nanosheet)-loaded dye with different irradiation times, percentage of photodegradation and pseudo-first-order plots: (a–c) UV light illumination and (d–f) visible light illumination.

A higher surface area with mesopores would allow more MG molecules to get adsorbed into the active sites under visible light irradiation. The performance of the UV illumination is relatively less due to the band gap excitation led possibility of photo-oxidation at the pores and interfaces. The kinetics of photocatalytic degradation of MG at the nanocatalyst (WS_2 nanosheets) surface can be evaluated qualitatively by employing the Langmuir–Hinshelwood (L–H) model [15].

The degradation trends of the MG dye can be found in figure 4.4 (b and e). Similarly, the curves of C_t/C_0 *vs*. t for different exposure conditions are shown in Figure 4.4 (c and f). The exponential decay trend would help to determine the pseudo-first-order rate constant, k_t involved in the reactions under UV and visible light illuminations. The k_t values are estimated as, 0.11 and 0.16 min^{-1}, respectively. An improved rate constant under visible light exposure suggests an improved photoactivity owing to induction of maximal redox reaction at the nanosheet surfaces through release and participation of free carriers, formation of superoxide radicals, etc. Moreover, the possibility of photo oxidation is largely avoided in this case, as compared to the UV photo-excitation condition.

4.3 Photcatalytic performance of WS_2/C-dot nanohybrid system

In order to investigate photoactivity of the as-synthesized WS_2/C dot hybrid system, we have chosen MO and MG dyes as the target agents under visible light illumination and considering different time duration of light exposure. The photoactivity of the WS_2/C-dot nanohybrid has been investigated after subjected to visible light illumination. Here the samples were prepared by adding 0.7 mg of the MG dye and an equal amount of MO dye (separately) to 50 ml of the 35% ethanol solution. The resultant sol was then placed inside a closed cabinet under visible light source. In this set up, the samples under study were placed on the base of the chamber, located at a vertical distance of 12 cm from the visible lamp (Philips, 15 W). The WS_2/C dot nanocatalyst loaded dye was irradiated under visible light for about 0, 15, 30, 45, 60 min. Next, 5 ml of the MG and MO solutions were taken for optical analysis knowing that, the peak maxima for the initial absorption of the MG appeared at ~617 nm, and for MO located at ~456 nm [8, 16]. In presence of the nano-catalyst, the percentage of decomposition of the MG and MO under visible light illumination for different time durations of the visible light exposure can be assessed from equation 4.1. It may be noted that, a suppression of the absorption response would indicate a proportionate lowering of the dye concentration in presence of the nanocatalyst. To draw insight from the photoactivity contribution arising due to the C-dots, experiment was conducted first on the bare WS_2 nanosheets and then on WS_2/C-dot nanohybrid systems. The UV-Vis optical absorption responses of the organic dyes and the nanocatalyst-loaded MO and MG systems can be found in Fig. 4.5 A and B (col.1). Recognizing untreated MO and MG peak maxima at ~456 nm and ~617 nm, as can be noticed, the absorbance shows a steady fall with increasing exposure time. Whereas, MO characterizes a broad spectral feature, MG gave a steep spectral response. Qualitatively, when exposed to visible light for time duration of 60 min, we obtained respective photodegradation efficiency of ~72.3% and 83.2% for the MO and MG dyes with inclusion of bare WS_2 nanosheets as photocatalyst (Fig. 4.5 A, col.2). However, the degradation efficacy

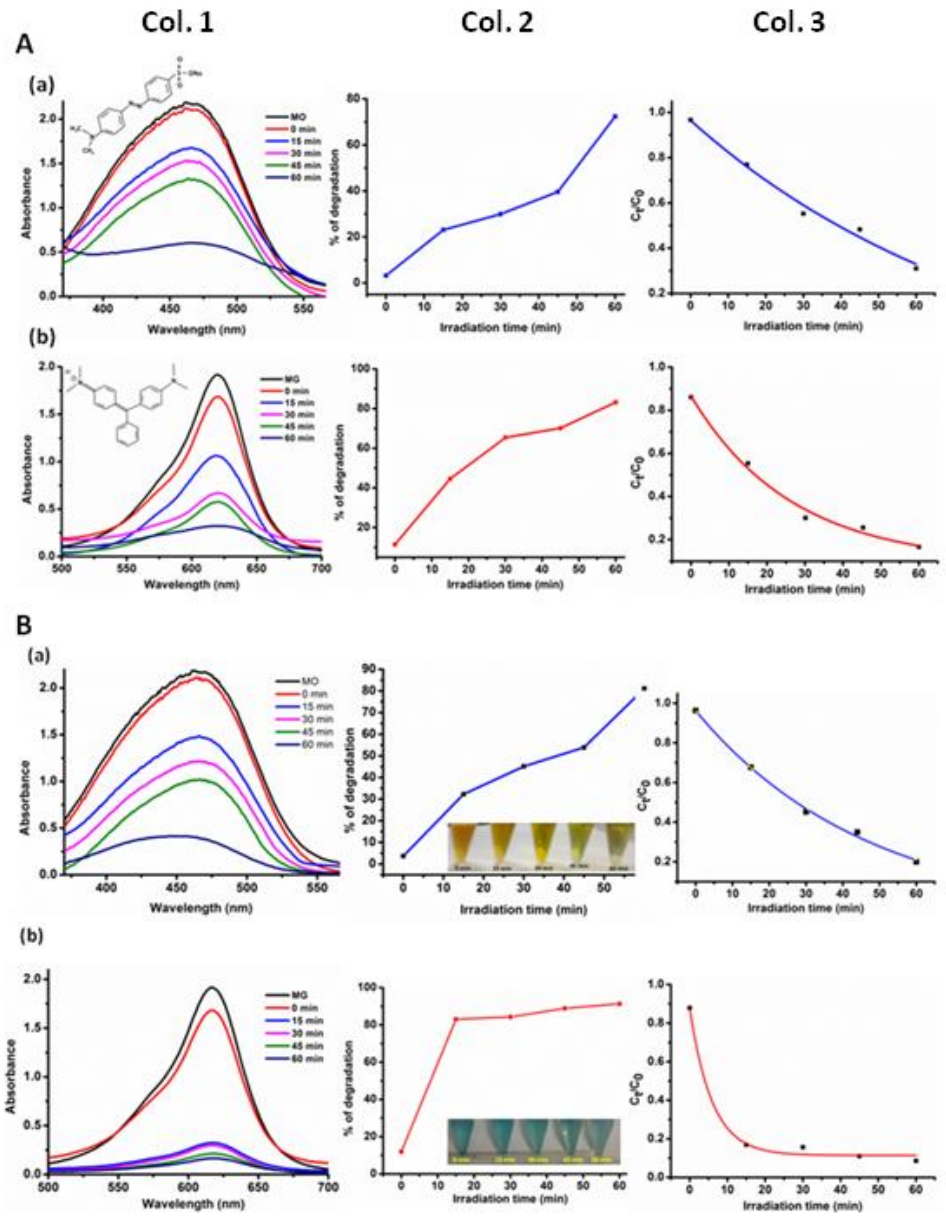

Figure 4.5: (A) Optical absorption spectral features illustrating photodegradation of (a) MO and (b) MG dyes under visible light illumination and using WS_2 nanosheets as the desired nanocatalyst. The exact nature of degradation with exposure time can be found in col.2 and col.3. (B) Optical absorption spectral features illustrating photodegradation of (a) MO and (b) MG dyes under visible light illumination and using WS_2/C-dots as the desired nanocatalyst. The exact nature of degradation with exposure time can be found in col.2 and col.3.

of the MO and MG dyes, in presence of WS_2/C-dot nanocatalyst was estimated to be, ~81.2% and ~91%; respectively (Fig. 4.5 B, col2). Moreover, the photodegradation response was seen to be much rapid in case of MG than the case for MO dye, possibly because of its strong sensitivity to the red part of the

visible light (Fig. 4.5, col. 2). It may be noted that, under similar conditions inorganic fullerene (IF) type and nanosheet based WS_2 systems could offer relatively lower MG degradation efficiencies, such as as high 71% and 86%.

The WS_2/C dot nanohybrid system has thus displayed an apparent increment in the photocatalytic activity. The C dots play an important role in enhancing the photoactivity of the 2D WS_2, which can be explained by the physiosorption process of the dye onto the WS_2 flakes [17]. Several environmental and chemical applications have been reported based on the physiosorption of organic aromatics onto the graphene systems [18, 19]. Normally when photons are incident on the WS_2 surfaces, the electrons are excited to the conduction band leaving aside the holes in the valence band. The deficiency of electron in the valence band of WS_2 can be filled by an incoming electron from the HOMO level of the dyes, which are in close proximity to the hybrid system [17]. As the process continues, the decomposition of the dye would take place until the thermodynamic equilibrium has been achieved. The schematic illustration for the degradation mechanism is shown in Fig. 4.6 (a,b).

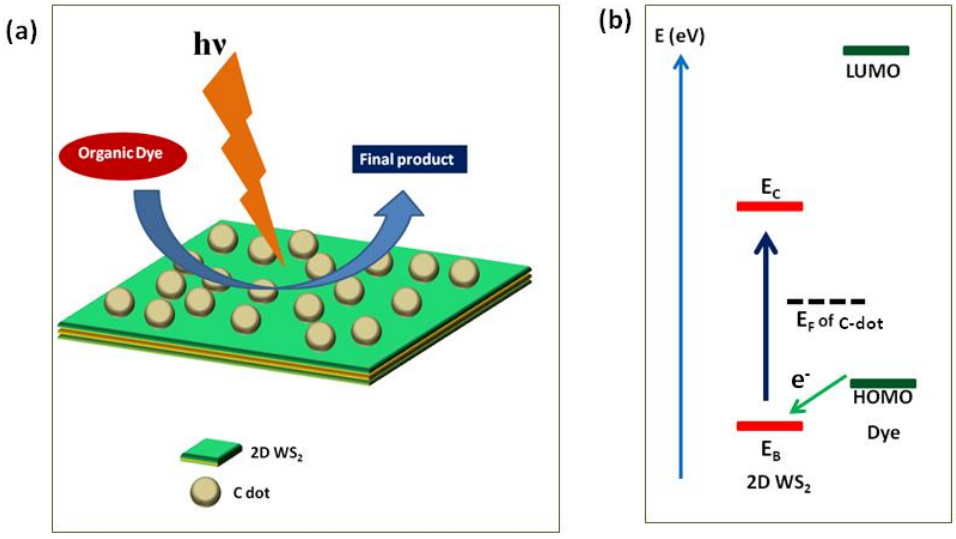

Figure 4.6: Schematic illustration of the photocatalytic activity: (a) degradation mechanism and (b) relevant energy scheme.

The nature of plots of C_t/C_0 versus t, are shown in Fig. 4.5A and 4.5B (col. 3). The plots essentially help to predict the pseudo first- order rate constant, k_a. To be specific, a higher rate constant predicts a higher amount of degradation of the target dye. The rate constants, as directly obtained from the nature of the curves and using the above equation, are estimated to be, 0.012 min^{-1} and 0.058 min^{-1} when MO and MG dyes were loaded with WS_2 nanosheets; respectively. In contrast, WS_2/C-dot loaded MO and MG systems gave respective k_a values as, 0.0215 min^{-1} and 0.168 min^{-1}. Apparently, the WS_2/C-dot nanohybrid is extremely sensitive to photoactivity as compared to its bare nanosheet counterpart.

4.4 Origin of enhanced bifunctional property of WS_2/C-dot systems

Bifunctionality of materials plays an important role in today's world. Modern technology always demands a device to be efficient not only in one application but more than one. It is well known that a material which is an efficient photocatalyst usually does not exhibit a good photoluminescence response. This is because for a photocatalytic reaction to occur there must be creation of electron hole pairs in order to restrict the recombination of these photogenarated electrons and holes [20]. Thus an ideal photocatalyst should have both a wide photoabsorption range and a high separation efficiency of the photogenerated charge carriers [20]. On the other hand, the luminescence property of a material arises as a result of the photogenerated electron-hole pairs. Carbon dot (C-dot) is a special class of material which can be used both as a photocatalyst and as an effective fluorescent material. The electron-transfer and capture properties of the C-dot provides a favourable condition to obstruct the recombination of the photogenerated charge carriers, resulting in enhanced photocatalytic performance. At the same time, C-dot possesses a wide absorption range excitation dependent photoluminescence property which can either be up converted or, down converted [20]. In our study, the C-dots have been adequately decorated over the WS_2 sheets and evaluated as a means of catalytic agent/fluorescent agent. An enhancement of both the photocatalytic and

photoluminescence characteristics of WS_2/C-dot nanohybrid system opens up new windows to search for new candidates which might offer a bifunctional property in ambient conditions.

4.5 Conclusion

The photocatalytic efficiency of the synthesized IF-type WS_2 nanocatalyst under visible light illumination gave a maximum degradation of 71.2% as compared to 45% when illuminated by the UV light. Moreover, the photodegradation efficiency of the WS_2 nanosheets for MG dye under visible light illumination was seen to be more effective than under the UV light condition. The band gap excitation led photo-oxidation might hinder the redox reactions at the nanocatalyst surface sites in the latter case. Finally, using the synthesized WS_2/C- dot nanocatalysts, photocatalytic degradation of MO and MG dyes were examined under visible light illumination. The degradation efficiency as high as, ~81.2% and 91% could be achieved against the respective target-dyes after an exposure time duration of 60 min. Among all the three investigated nanocatalysts, WS_2/C dot system exhibited a better and excellent photocatalytic response.

References:

[1] Chhowalla, M., Suk Shin, H., Eda, G., Li, L-J., Loh, K. P., Zhang, H. The chemistry of two-dimensional layered transition metal dichalcogenide nanosheets. *Nature Chemistry*, 5:263-275, 2013.

[2] Vattikuti, S. V. P., Byon, C., Reddy, C. V. Preparation and improved photocatalytic activity of mesoporous WS_2 using combined hydrothermal-evaporation induced self-assembly method. *Materials Research Bulletin*, 75:193–203, 2016.

[3] Mishra, A.K., Lakshmi, K.V., Huang, L. Eco-friendly synthesis of metal dichalcogenides nanosheets and their environmental remediation potential driven by visible light. *Scientific Reports,* 5:15718, 2015

[4] Sang, Y., Zhao, Z., Zhao, M., Hao, P., Leng, Y., Liu, H. From UV to near-infrared, WS_2 nanosheet: a novel photocatalyst for full solar light spectrum photodegradation. *Advanced Materials*, 27:363–369, 2015.

[5] Vattikuti, S.V.P., Byon, C., Reddy, C.V., Ravikumar, R.V.S.S.N. Improved photocatalytic activity of MoS_2 nanosheets decorated with SnO_2 nanoparticles. *RSC Advances*, 5:86675–86684, 2015.

[6] Srivastava, S., Sinha, R., Roy, D. Toxicological effects of malachite green, *Aquatic Toxicology*, 66:319- 329, 2004.

[7] Eumann, M., Schaeberle, C. Water. *Brewing Materials and Processes,* ISBN: 0128004681, pages 97–111, Academic Press, 2016.

[8] Rabieh, S., Bagheri, M., Heydari, M., Badiei, E. Microwave assisted synthesis of ZnO nanoparticles in ionic liquid [Bmim] cl and their photocatalytic investigation. *Materials Science in Semiconductor Processing*, 26:244, 2014

[9] Paul, N., Deka, A., Mohanta, D. Augmented photocatalytic activity and luminescence response of Tb^{3+} doped nanoscale titania systems. *Journal of Applied Physics,* 116:144902-1-7, 2014.

[10] Hazarika, S.J., Mohanta, D. Inorganic fullerene-type WS_2 nanoparticles: processing, characterization and its photocatalytic performance on malachite green. *Applied Physics A*, 123:381-391, 2017.

[11] Bingham, S., Daoud, W.A. Recent advances in making nano-sized TiO_2 visible-light active through rare-earth metal doping. *Journal of Material Chemistry,* 21:2041-2050, 2011.

[12] Peng, T., Zhao, D., Song, H., Yan, C. Preparation of lanthana-doped titania nanoparticles with anatase mesoporous walls and high photocatalytic activity. *Journal of Molecular Catalalysis A*, 238:119-126, 2005.

[13] Rapoport, L., Bilik, Y., Feldman, Y., Homyonfer, M., Cohen, S.R., Tenne, R. Hollow nanoparticles of WS_2 as potential solid-state lubricants. *Nature*, 387:791–793, 1997.

[14] Vattikuti, S.V.P., Byon, C., Chitturi, V. Selective hydrothermally synthesis of hexagonal WS_2 platelets and their photocatalytic performance under visible light irradiation. *Superlattices Microstructures*, 94:39–50, 2016.

[15] Gaya, U.I., Abdullah, A.H. Heterogeneous photocatalytic degradation of organic contaminants over titanium dioxide: a review of fundamentals, progress and problems. *Journal of Photochemistry and Photobiology C*, 9:1–12, 2008.

[16] Zhang, W., Xiao, X., Zheng, L., Wan, C. Fabrication of TiO_2/MoS_2@zeolite photocatalyst and its photocatalytic activity for degradation of methyl orange under visible light. *Applied Surface Science*, 358:468 -478, 2015.

[17] Atkin, P., Daeneke, T., Wang, Y., Carey, B.J., Berean, K.J., Clark, R.M., Ou, J.Z., Trinchi, A., Cole, I.S., Kalantar-zadeh, K. 2D WS_2/carbon dot hybrids with enhanced photocatalytic activity. *Journal of Material Chemistry A*, 4:13563-13571, 2016.

[18] Yang, K., Chen, B., Zhu, L. Graphene-coated materials using silica particles as a framework for highly efficient removal of aromatic pollutants in water. *Scientific Reports*, 5:11641, 2015.

[19] Ramesha, G.K., Vijaya Kumara, A., Muralidhara, H.B., Sampath, S. Graphene and graphene oxide as effective adsorbents toward anionic and cationic dyes, *Journal of Colloids and Interface Science*, 361:270- 277, 2011.

[20] Zhang, Z., Zheng, T., Li, X., Xu, J., Zeng, H. Progress of Carbon Quantum Dots in Photocatalysis Applications. *Particle and Particle Systems Characterization, 33*:457–472, 2016.